

The effect of a small amount of impurity on the oxidation of Si_3N_4 ceramics

Y. UKYO

Toyota Central Research and Development Laboratories Inc., Nagakute-cho, Aichi-gun, Aichi, 480-11 Japan

To investigate the effect of a small amount of impurity, especially $\text{Ca}(\text{CaO})$, on the oxidation of Si_3N_4 ceramics at high temperatures, two kinds of Si_3N_4 ceramics with different amounts of impurities were fabricated. The decrease in the strength of Si_3N_4 ceramics containing calcium as an impurity became severe when oxidation time was longer and temperature was higher. The decrease in the strength was caused by the formation of pits. It is estimated that pits are formed due to the high concentration of calcium in the oxidized layer near to the pits.

1. Introduction

Si_3N_4 ceramics is potentially suitable for high-temperature engineering applications, particularly for use in automobile engines because of its excellent mechanical properties, such as high-temperature strength or high fracture toughness. However, the degradation of Si_3N_4 ceramics due to high-temperature oxidation will become a serious problem when Si_3N_4 ceramics are used at high temperature. Extensive studies have been reported on the oxidation of Si_3N_4 ceramics at high temperature by many authors [1]. Pure Si_3N_4 shows excellent resistance to high-temperature oxidation and is stable up to 1400–1600 °C in air [2–4]. This excellent resistance is attributed to the formation of a pure SiO_2 or Si_2ON_2 layers which act as protective layers [5, 6]. Some kinds of oxides and nitrides, such as Y_2O_3 , Al_2O_3 and AlN , are used as sintering additives for Si_3N_4 -based ceramics, because Si_3N_4 has poor sinterability due to its strong covalent bonding [7]. Most of these sintering additives will form a liquid phase during sintering by reaction with SiO_2 which exists on the Si_3N_4 powders, and this remains at the grain boundaries as glassy phases after sintering. When the Si_3N_4 ceramics containing glassy phases are oxidized at high temperature, the constituents of the additives will diffuse towards the surface through the grain boundaries and react with the SiO_2 film formed on the surface by the reaction with Si_3N_4 matrix and oxygen. As a result of this reaction, SiO_2 will cease to be a protective layer and then oxidation will proceed. Sometimes, the strength rapidly decreases due to the formation of pits or voids at the interface of the oxidized layer and matrix [7, 8]. When MgO is used as a sintering additive, the formation of pits or voids is often observed [8–11].

In this study, the effect of a small amount of $\text{Ca}(\text{CaO})$, which is contained in Si_3N_4 powder as an impurity, on the high-temperature oxidation, was investigated in detail.

2. Experimental procedure

Two kinds of Si_3N_4 powders were used in this study. They differed in the amounts of impurities contained such as iron, calcium and aluminium, as shown in Table I. Powder A contained in the order of 1300–2300 p.p.m. (in mass) of iron, calcium and aluminium, while powder B contained a very small amount of impurity. Y_2O_3 (4 mass %) and Al_2O_3 (2 mass %) were used as sintering additives. These powders were milled in ethanol for 24 h and then sintered at 1850 °C for 4 h in a nitrogen atmosphere. Bending test specimens with dimensions 3 mm × 4 mm × 40 mm, were cut from the sintered bodies and used for the high-temperature oxidation test. The surfaces of the specimens were ground by a diamond wheel with 600 grid. Specimens A and B were made of powders A and B, respectively.

The oxidation test was performed at 1000, 1100 and 1200 °C for up to 720 h in static air. For each oxidation test, 20 specimens were used. After the oxidation test, weight change was measured and products were determined by the X-ray diffraction method, and compositional change near the surface was determined by electron probe microanalysis (EPMA) and SEM-EDX. The bending strength at room temperature before and after oxidation was measured and the fracture surfaces of all the specimens were observed by scanning electron microscopy (SEM) to identify the fracture origins.

3. Results and discussion

3.1. Weight change

Fig. 1 shows the weight change during oxidation. Each point shows an average value of 20 specimens. The weight increased with time and temperature, especially at 1200 °C. No difference in weight change between specimens A and B was observed, as shown in Fig. 1. Thus, the effect of the impurities on the oxidation cannot be estimated by the weight gain.

3.2. Observation of surface morphology

Fig. 2 shows surface morphologies before and after oxidation at 1000, 1100 and 1200 °C for 720 h. Fig. 2a–d show the surface of specimen A which contains a large amount of impurities. Many grinding traces were observed before oxidation. After oxidation

TABLE I Impurities p.p.m. (in mass) of Si₃N₄ powders used in this study

	O	Fe	Ca	Al
Powder A	2400	1300	2300	2000
Powder B	1180	15	2.1	11

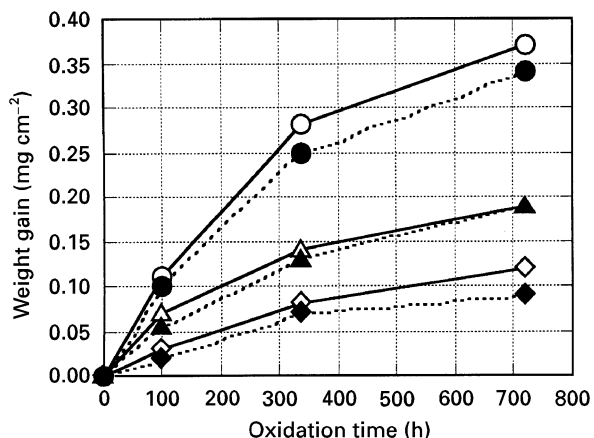


Figure 1 The dependence of weight change of specimens (◇, △, ○) A and (◆, ▲, ●) B on oxidation time and temperature: (◇, ◆) 1000 °C, (△, ▲) 1100 °C, (○, ●) 1200 °C.

at 1000 °C for 720 h, most of the traces had disappeared and the surface was covered with an oxidation layer. Granular crystals were observed on the surface. At 1100 °C, prismatic crystals were observed in addition to the granular crystals, and the traces of grinding had completely disappeared. The surface seems to be covered by a thick oxidized layer and the prismatic crystals have grown into 20–50 μm. There were many cracks which were thought to be formed during the cooling process, both at 1100 and 1200 °C. The granular and prismatic crystals formed were identified by the X-ray diffraction methods as α-SiO₂ and Y₂Si₂O₇, respectively. This suggests that the oxidized layer is composed mainly of SiO₂ at lower temperature or in the initial stage of oxidation, and the Y₂Si₂O₇ is then formed by the reaction of SiO₂ with Y (Y₂O₃) which migrates through the grain boundaries to the surface. Y₂Si₂O₇ is usually formed during oxidation of Si₃N₄ ceramics containing Y₂O₃ (12, 13, 15).

Fig. 2e–h show the surface of specimen B. The change in the surface morphology is basically similar to that of specimen A, except that the traces of grinding are left at 1100 °C, and that Y₂Si₂O₇ crystals formed in specimen B are smaller than those in specimen A. The compositions of the surface were analysed by fluorescence X-ray and SEM-EDAX to investigate the difference in surface morphology between specimens A and B after oxidation. The mean calcium concentration at the surface of specimen A rapidly increased with increasing temperature and time, as shown in Fig. 3, while the concentrations of iron, yttrium and aluminium slightly increased. Therefore, the oxide layer may be composed of α-SiO₂, Y₂Si₂O₇

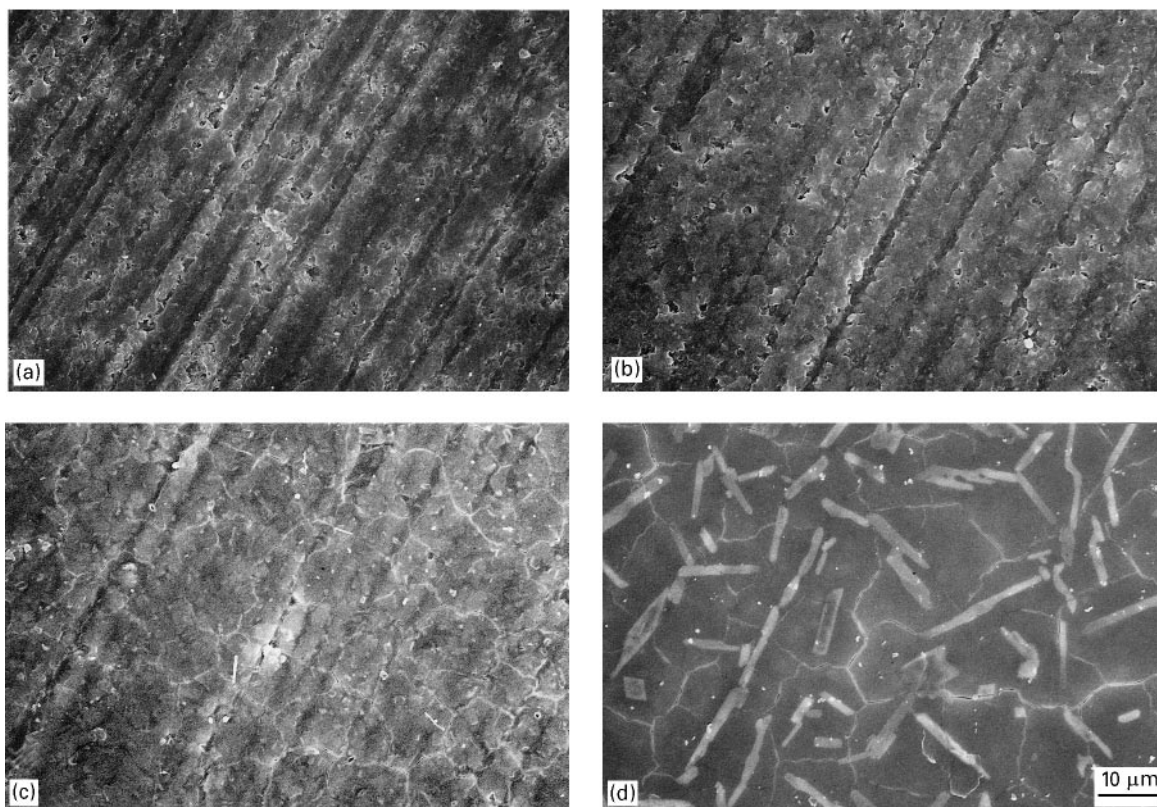


Figure 2 Surface morphologies of specimens (a–d) A and (e–h) B, (a, e) before, and after oxidation for 72 h at (b, f) 1000 °C, (c, g) 1100 °C and (d, h) 1200 °C.

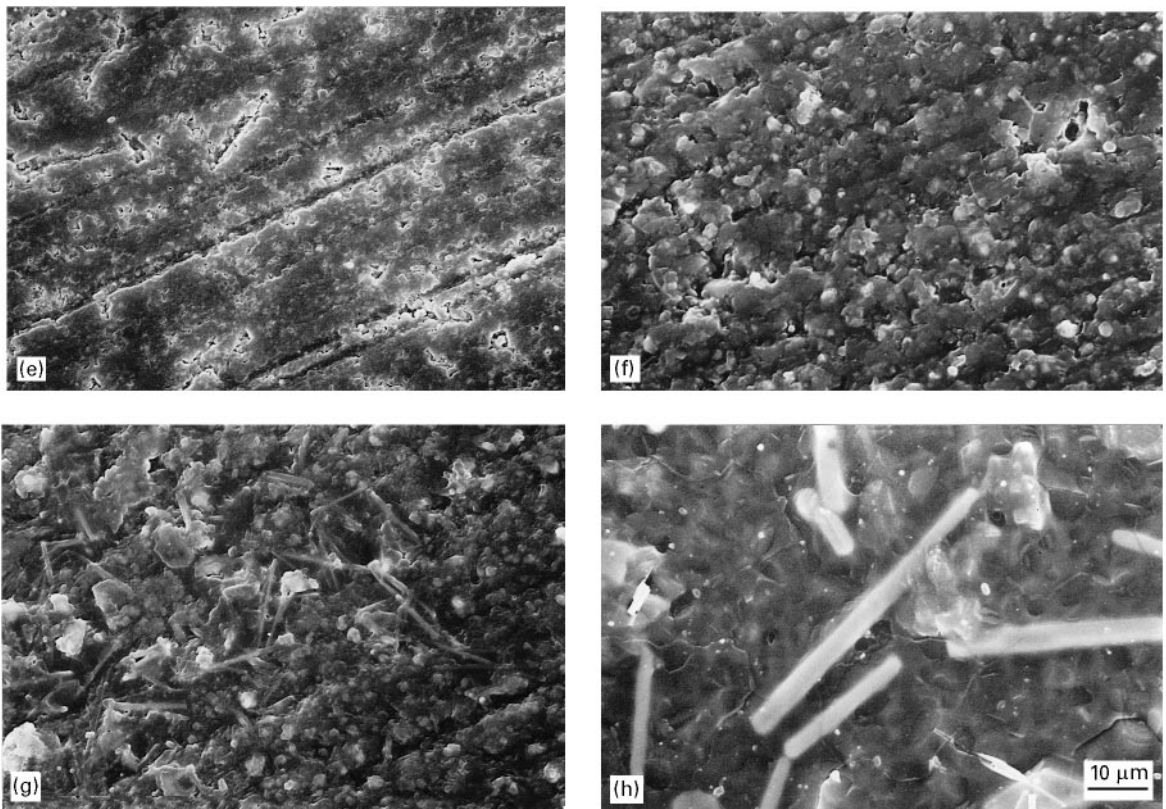


Figure 2 (Continued)

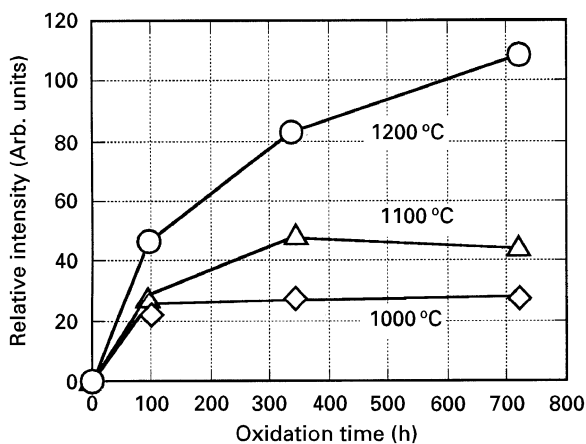


Figure 3 Dependence of calcium concentration at the surface of specimen A on oxidation time and temperature (fluorescence X-ray analysis).

and a glassy phase containing a large amount of Ca(CaO). Fig. 4 shows the results of the composition analysis by SEM-EDX of the surface of specimen A oxidized at 1200 °C for 720 h. The calcium concentration near prismatic $Y_2Si_2O_7$ crystals is very high, as shown in Fig. 4. Therefore, the prismatic $Y_2Si_2O_7$ crystals may grow in the glassy phase with high Ca(CaO) content, that is, lower melting point. On the other hand, $Y_2Si_2O_7$ crystals formed on the surface of specimen B were smaller than those formed on the surface of specimen A. These results reveal that calcium, which is contained in Si_3N_4 powder as an impu-

rity, has a large influence on the surface morphology of the specimen after oxidation.

3.3. Strength after oxidation

Fig. 5a and b show the room-temperature strength after oxidation. Each point shows the average of 20 specimens. The strengths of specimens A and B before oxidation were about 800 and 900 MPa, respectively. The strength of specimen A after oxidation decreased with oxidation time and with increasing temperature. For example, the strength after oxidation for 720 h at 1200 °C became about 50% of that before oxidation.

On the other hand, the strength of specimen B after oxidation slightly decreased in earlier stages of oxidation and was independent of oxidation time and temperature. This result shows that the impurities contained in Si_3N_4 ceramics have a large effect on not only the surface morphology but also the strength after oxidation.

The fracture surface of all the specimens was observed by scanning electron microscopy (SEM) to identify the fracture origins and to investigate the effect of the impurities on the strength after oxidation. Fig. 6a–j show the typical fracture origins of specimens A and B, respectively. The fracture origin of specimen A before oxidation was mostly defects such as voids, as shown in Fig. 6a–e, which are thought to be introduced during processing. When the oxidation temperature is above 1100 °C, the fracture origin changed from the defects mentioned above into the pits formed during oxidation. Table II shows the

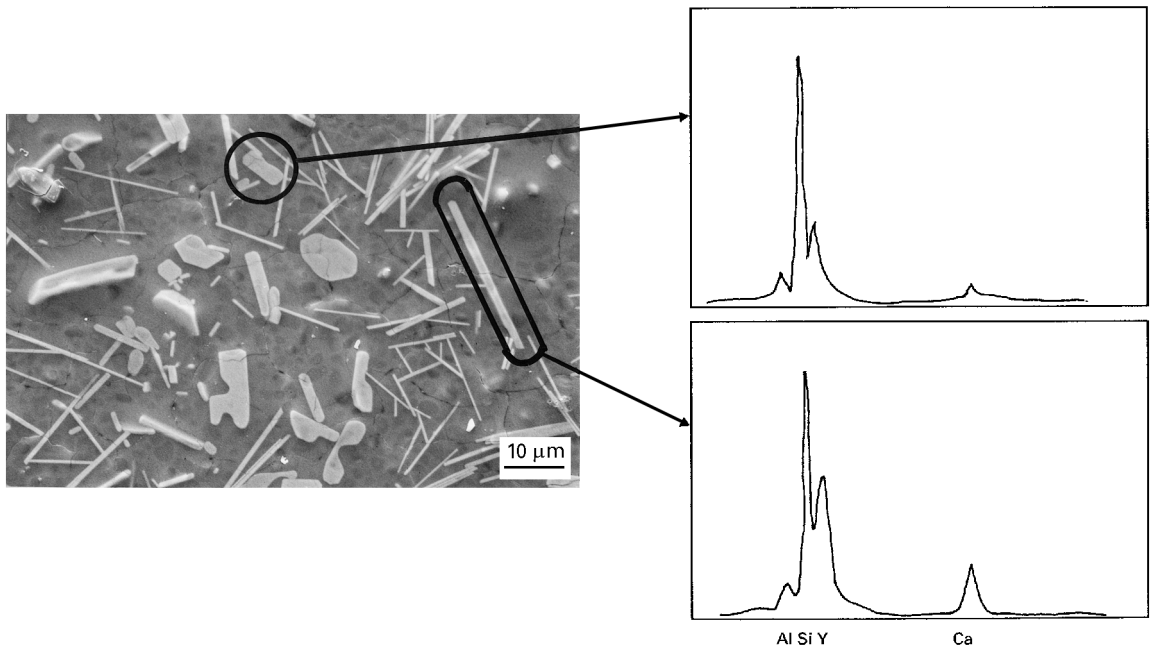


Figure 4 Surface morphology of specimen A after oxidation at 1200 °C for 720 h and the EDAX spectra near a $Y_2Si_2O_7$ crystal.

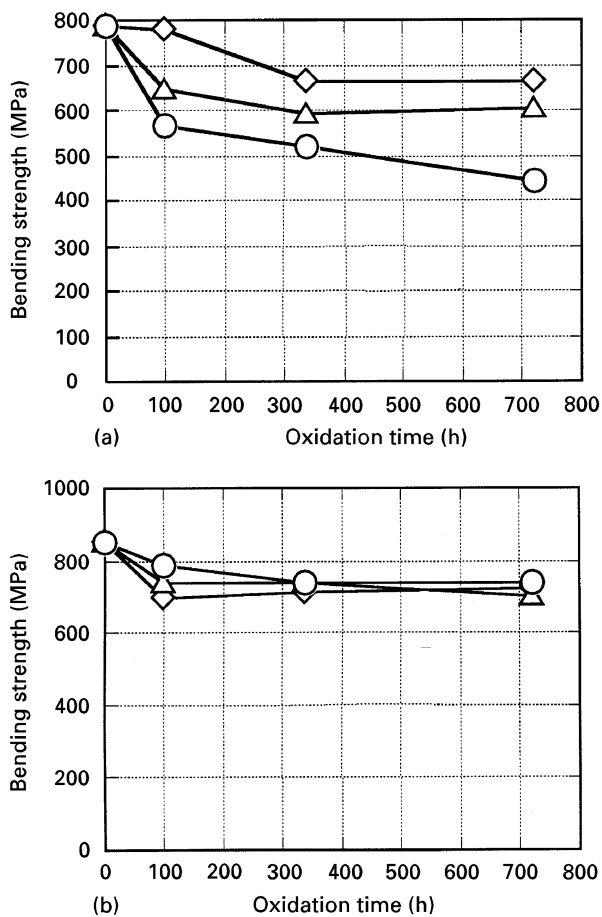


Figure 5 Bending strength of specimens (a) A and (b) B, at room temperature after oxidation at (◇) 1000 °C, (△) 1100 °C, (○) 1200 °C.

number of specimens for which pits were the fracture origin. As the oxidation temperature increases and the oxidation time becomes longer, the number of specimens for which fracture origin are pits increased rapidly. The fracture origin of all the specimens after oxidation at 1200 °C for 720 h was pits.

These pits are often observed when Si_3N_4 ceramics containing magnesium oxide (MgO) are oxidized at high temperatures [9, 10]. In this case, the magnesium oxide exists as a glassy phase at grain boundaries. Magnesium diffuses towards the surface and then dissolves into the oxidized layer at the surface, resulting in an increase in magnesium concentration in the oxidized layer [16]. For example, it is reported that the concentration of MgO in the oxidized layer of Si_3N_4 with 1 mass % MgO was about 26 mass %. It is thought that the pit is formed due to dissolution of the Si_3N_4 matrix into the oxidized layer containing a large amount of magnesium oxide [14].

The concentration profile of calcium (CaO) was measured by EPMA to elucidate the reason for the formation of pits. Fig. 7 shows the calcium concentration profile of the specimen oxidized at 1200 °C for 720 h. The concentration of calcium in the oxidized layer is very much higher than that in the matrix. This means that calcium diffuses towards the surface and dissolves into the oxidized layer as does magnesium. Fig. 8 shows the calcium concentration determined by EDAX in the oxidized layer near the pit in the same specimen as in Fig. 7. The concentration of calcium in the oxidized layer near the pits was about 18 mass %, in the form of calcium oxide (CaO).

The concentration of calcium in the oxidized layer near a pit is extremely high and therefore there is a strong correlation between the formation of pits and the concentration of calcium. The dissolution of calcium or calcium oxide decreases the melting point of the oxidized layer composed of mainly SiO_2 and increases the basicity. The increase in the basicity enhances the dissolution of N_2 and therefore, the pits are thought to be formed by the local dissolution of Si_3N_4 into the oxidized layer [17].

Fig. 9 shows the dependence of the mean size of a pit in specimen A on oxidation time and temperature. The pit size becomes larger with time and with

increasing temperature. The decrease in the strength of specimen A after oxidation is thought to be due to the formation of a pit and depends on the size of the pit. Attention must be paid to small amounts of calcium contained as impurities, because the pit will be formed easily and the strength will decrease during oxidation at high temperature.

TABLE II Number of specimens fractured due to the formation of pits

Temperature (°C)	Oxidation time (h)		
	100	336	720
1000	0	0	0
1100	3	14	6
1200	12	19	20

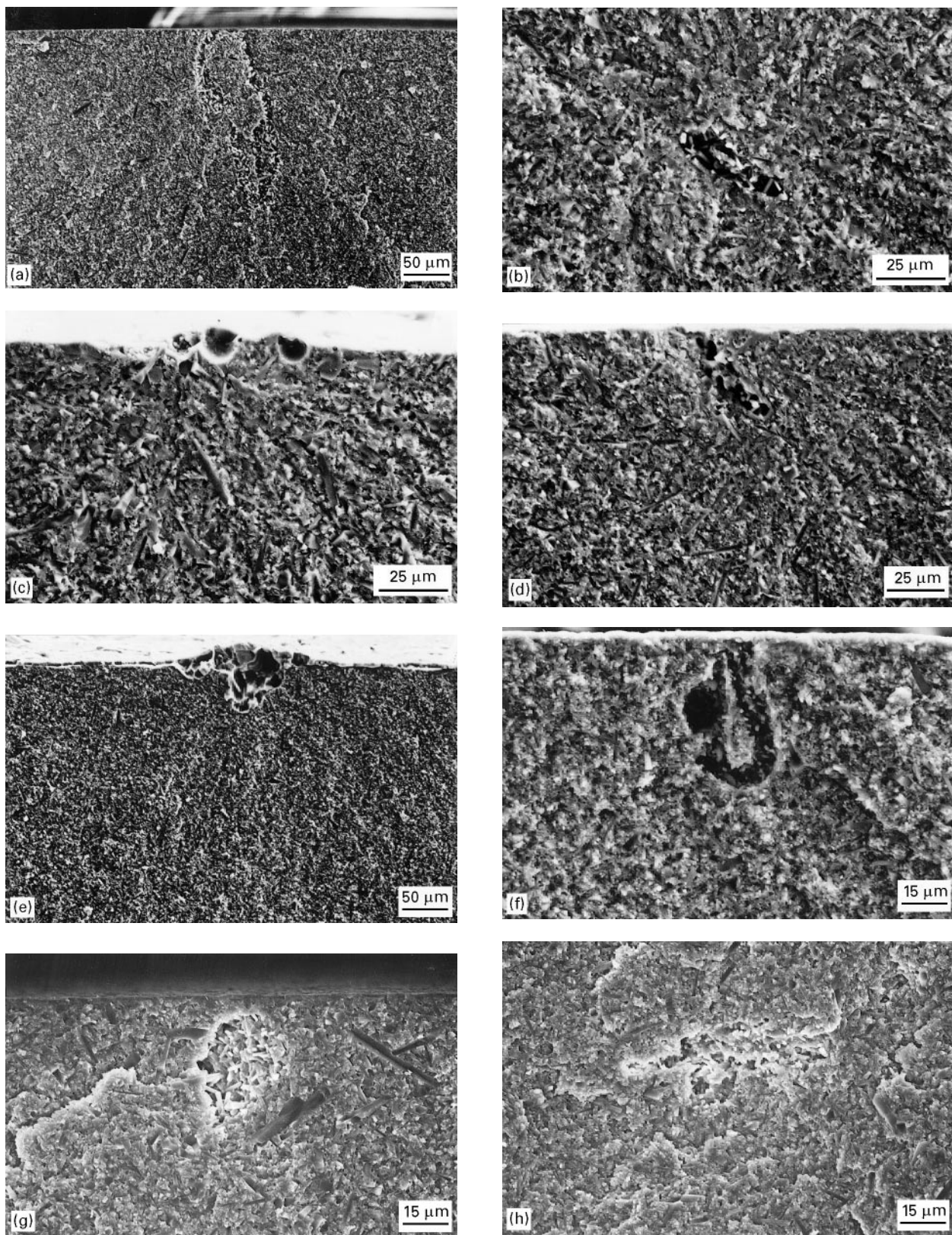


Figure 6 Fracture surfaces of specimens (a–e) A and (f–j) B, (a, f) before, and after oxidation for 720 h at (b, g) 1000 °C, (d, i) 1100 °C, (e, j) 1200 °C, and (c, h) for 336 h at 1100 °C.

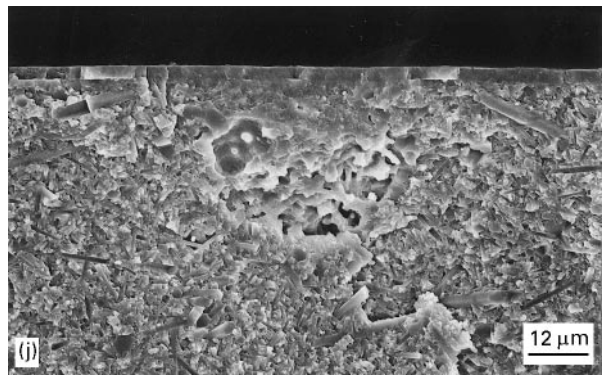
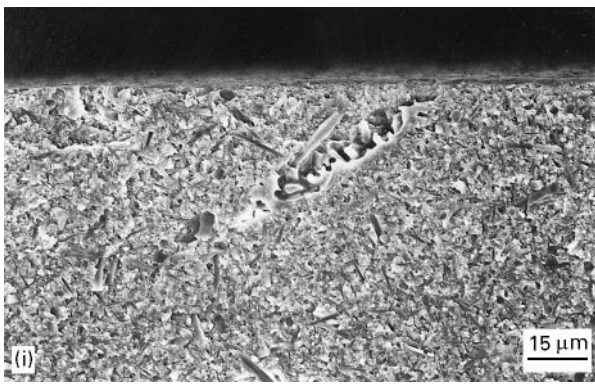


Figure 6 (Continued)

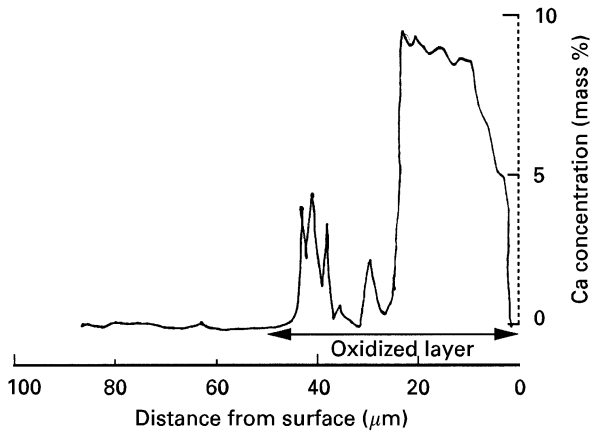


Figure 7 Compositional change near the surface of specimen A after oxidation at 1200 °C for 720 h.

4. Conclusions

The effect of a small amount of impurity, especially calcium or calcium oxide, on the oxidation of Si_3N_4 ceramics has been investigated using two kinds of Si_3N_4 ceramics consisting of Si_3N_4 powders and different amounts of impurities. The oxidation test was performed in static air at 1000, 1100 and 1200 °C for up to 720 h. The following results have been obtained.

1. $\alpha\text{-SiO}_2$ and $\text{Y}_2\text{Si}_2\text{O}_7$ were formed as crystalline phases in the oxidized layer. $\text{Y}_2\text{Si}_2\text{O}_7$ grew into large grains in the region where the concentration of calcium was higher.
2. The weight change during oxidation was independent of the amount of impurities.
3. The concentration of calcium in the oxidized layer of the specimen containing a large amount of calcium as an impurity increased with oxidation time and temperature.
4. The decrease in the strength of Si_3N_4 ceramics containing calcium as an impurity became severe when the oxidation time was longer and the temperature was higher. The decrease in strength was caused by the formation of pits.
5. It is estimated that pits are formed due to high concentration of calcium in the oxidized layer, because the oxidized layer near pits contains a large amount of calcium.

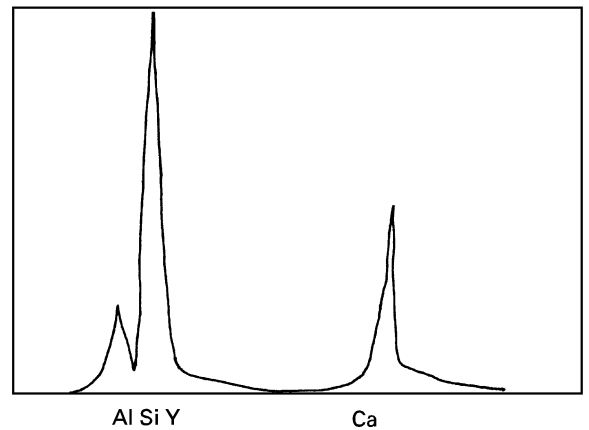
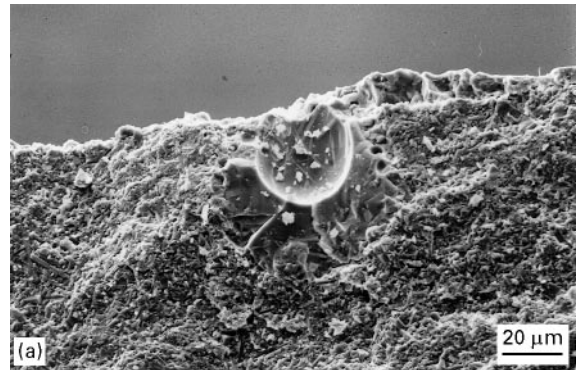


Figure 8 (a, b) EDX spectra near the pit of specimen A after oxidation at 1200 °C for 720 h.

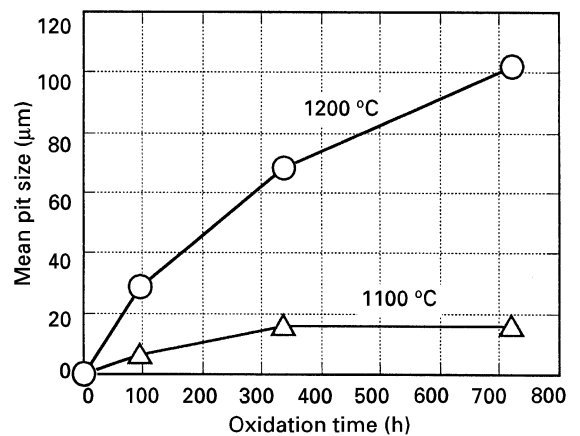


Figure 9 Dependence of mean pit size on oxidation time and temperature.

References

1. S. C. SINGHAL, in "Nitrogen Ceramics", edited by F. L. Riley (Noordhoff, NATO, Lyden NL, 1977) p. 607.
2. F. GALASSO, U. KUNTZ and W. J. CROFT *J. Amer. Ceram. Soc.* **55** (1972) 431.
3. I. FRANZ and W. LANGHEINRICH, *Solid Electron.* **14** (1971) 499.
4. T. HIRAI and K. NIIHARA and T. GOTO, *J. Amer. Ceram. Soc.* **63** (1980) 419.
5. L. U. J. T. OGBUJI, *ibid.* **75** (1992) 2995.
6. H. DU. R. E. TRESSLER, K. E. SPEAR and C. G. PANTANO, *J. Electrochem. Soc.* **136** (1989) 1527.
7. G. PETZOW and P. GREIL, in "Proceedings of the International Symposium on Ceramic Components for Engines", edited by S. Somiya, E. Kanai and K. Ando (KTK Scientific, Tokyo, 1983), p. 177.
8. S. C. SINGHAL, *J. Mater. Sci.* **11** (1976) 500.
9. W. C. TRIPP and H. C. GRAHAM, *J. Amer. Ceram. Soc.* **59** (1976) 399.
10. C. CM. WU, K. R. MCKINNEY, R. W. RICE, W. J. McDONOUGH and S. W. FREIMAN, *J. Mater. Sci.* **16** (1981) 3099.
11. R. W. KOSSOWSKY, *ibid.* **8** (1973) 1603.
12. D. CUBICCIOTTI and K. H. LAU, *J. Amer. Ceram. Soc.* **61** (1978) 512.
13. G. Q. WEAVER and J. W. LUCEK, *Amer. Ceram. Soc. Bull.* **57** (1978) 1131.
14. D. CUBICCIOTTI and K. H. LAU, *J. Amer. Ceram. Soc.* **126** (1979) 1723.
15. G. N. BANIBI, A. BELLOSI and P. V. VINCENZINI, *J. Mater. Sci.* **19** (1984) 1029.
16. F. F. LANGE and D. R. CLARKE, *J. Amer. Ceram. Soc.* **63** (1980) 586.
17. E. A. DANCY and D. JANSSEN, *Canad. Metall. Quart.* **15** (1976) 103.

*Received 8 December 1995
and accepted 10 March 1997*